J Stat Phys (2011) 144:219–240
DOI 10.1007/s10955-011-0251-6

Molecular and Functional Aspects of Bacterial Chemotaxis

A. Celani · T.S. Shimizu · M. Vergassola

Received: 27 January 2011 / Accepted: 12 June 2011 / Published online: 30 June 2011

Abstract We consider the dynamics of chemotaxis in the model bacterium *Escherichia coli*. We analyze both its molecular mechanisms and the functional causes governing the evolution of the observed behaviors. We review molecular models of the transduction network controlling the bacterial chemotaxis in response to chemoattractant binding to the receptors. In particular, recent progress stimulated by FRET experiments is presented for statistical physics allosteric models. The response function to a pulse of chemoattractant is expressed in terms of microscopic parameters of the allosteric models. The functional causes for the shape of the response function, as measured in experimental tethering assay, are then investigated. A hydrodynamic equation, valid for space-time scales larger than the microscopic running length and time, is derived for the position of a swimming bacterium. It is then shown how optimization over the microscopic parameters of the response function yields the curve observed experimentally. In particular, the observed property of adaptation to the background level of aspartate emerges as being produced by fluctuations in the space-time chemoattractant profiles sensed by bacteria along their trajectories. This functional cause is distinct from arguments based on the extension of the dynamical range. Future directions and experiments to probe the adaptation of *E. coli* chemotaxis to the environmental conditions and its response to realistic space-time chemoattractant stimuli are finally discussed.

Keywords Bacterial chemotaxis · Adaptation · Hydrodynamic limit · Homogenization methods

A. Celani · M. Vergassola (✉)
Research Unit "Physics of Biological Systems" and CNRS, URA 2171, Institut Pasteur, 28 rue du Dr Roux, 75724 Paris Cedex 15, France
e-mail: massimo.vergassola@pasteur.fr

T.S. Shimizu
FOM Institute for Atomic and Molecular Physics (AMOLF), Science Park 104, 1098 XG Amsterdam, The Netherlands

1 Introduction

The ability to orient and actively move towards convenient locations is one of the hallmarks of living organisms. A wide variety of mechanisms of motility have then emerged throughout natural evolution and they turn out to be affected by the physical conditions experienced by the organism. The motion of prokaryotic bacteria is driven by a wide variety of environmental stimuli, such as light (phototaxis), electric fields (galvanotaxis), magnetic fields (magnetotaxis), temperature (thermotaxis) and concentration of chemicals (chemotaxis). Our focus here will be concentrated on the latter, whereby bacteria are able to ascend gradients of chemoattractants or escape from chemorepellents (see [1] for an excellent introduction).

Orientation of bacteria, namely of the model organism *E. coli*, must overcome challenges imposed by their typical size, of the order of microns. On the one hand, this microscopic size makes individual bacteria unable of keeping a straight course, which is continuously deviated by molecular diffusion. The resulting curvature effects of the bacterial runs are quantified by rotational diffusion, which is measured to be of the order of 0.1 $\mathrm{rad}^2/\mathrm{s}$. In other words, the rotational diffusion leads to a standard deviation of 30° over a typical duration of the runs of about 2 s. Runs correspond to the counterclockwise rotation of the curled bacterial flagella, which is randomly interrupted by short periods of clockwise rotation, lasting for about 0.1 s. Clockwise rotations of one or several flagella induce the tumbling of the bacteria, i.e. the random reorientation of their running direction (we refer to [1] for more details). The combined effect of rotational diffusion and the tumblings is that the bacterial motion in the absence of any chemoattractant is indistinguishable from a random walk on time scales of a few run/tumble events. On the other hand, the microscopic size of *E. coli* ensures that the Reynolds and the Péclet numbers are very small on the scale of individual bacteria. The consequence is that local gradients of chemical concentration do exist and provide, if properly measured (see the sequel), a reliable cue for orientation. This situation is to be contrasted with that of macro-organisms, such as insects, where the typical length scales are orders of magnitude larger (see [2] for consequences on the diffusion of chemicals and motility).

The smallness of the Péclet number at the single cell scale has made that most theoretical and experimental work concentrated until recently on the chemotactic response to relatively simple signals, such as pulses, steps and static gradients. In fact, the relatively high speed of *E. coli* (several body lengths/second) implies that the bacterium can cover much larger distances in the typical velocity decorrelation timescale of a few runs and tumbles. It is also relevant to remark that experiments [3, 4] show that the peak of bacterial motility for colonies grown in the laboratory is achieved when colonies are dense, i.e. when the concentration of chemoattractants is strongly perturbed by the presence of surrounding bacteria (see also [5]). It is therefore of high interest to build upon previous results and start probing the chemotactic response to signals having more complex space-time structures, more directly related to the environmental wild conditions. This has the double scope of assaying the molecular response of the system and exploring the functional consequences and the evolutionary forces that lead to the emergence of the experimentally observed bacterial behaviors. This is the line of research which we pursued in recent publications [6–8]. Our scope here is to report progress along these lines by reviewing previous work, by discussing recent and new results and finally by presenting open problems and future directions.

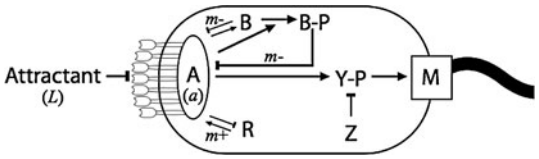

Fig. 1 The *E. coli* chemotaxis signaling network. The input ligand concentration, L, is sensed by the membrane-associated receptor-kinase complex, A, to regulate its autophosphorylation activity, a. A then transfers phosphate to the response regulator, CheY (Y), the phosphorylated form of which (Y-P) interacts with the flagellar motor (M), to control swimming behavior. The feedback loop is closed by the methyltransferase CheR (R) and the methylesterase/deamidase CheB (B), by regulation of the receptor methylation level, m. CheZ (Z), the phosphatase for CheY-P, decreases the signal lifetime, thus accelerating the response of the pathway

2 Molecular Implementation of Chemotaxis Signaling

2.1 Signaling Network

In the most intensively studied species, *E. coli*, the chemotaxis signaling network has a relatively simple topology (Fig. 1; for a recent review on chemotaxis signaling, see [9]). A population of receptors at the cell surface bind chemoeffector ligands and affect the rate at which an intracellular kinase, CheA, hydrolyzes ATP on a time scale ∼0.1 s. The phosphate group produced in this hydrolysis reaction is then passed to a response regulator protein, CheY, which affects stochastic switches in motor rotation direction (CCW or CW) on a time scale ∼1 s.

The receptor-kinase complex is stable on the time scale of the response, and hence can be considered a single molecular species in considering signaling function. In addition to the input ligand concentration, L, the receptor-kinase activity, a, is modulated by chemical modifications at specific amino acid residues of the receptor cytoplasmic domains. These covalent modifications are catalyzed by two enzymes: CheR, which adds methyl groups, and CheB, which removes them. The balance between the activity of these two enzymes determines the average methylation level, m, which can take values between 0 and a maximal value, M, corresponding to the number of modification sites per receptor monomer (4 for the aspartate receptor Tar). Thus, the kinase activity, a, is determined by a function of both of these variables, $a = G(L, m)$.

Kinase activity decreases with attractant ligand concentration ($\partial G/\partial L < 0$), and increases with methylation ($\partial G/\partial m > 0$). The activities of both CheR and CheB, which determine the dynamics of m, in turn, depend on the kinase activity, a, in a manner that provides negative feedback. These reactions occur on a much slower time scale (∼10 s) than that of the modulation of a, so these dynamics must be considered explicitly, and in general can be written as

$$\frac{dm}{dt} = F(a, m, L). \tag{1}$$

Transmission of changes in a to the motor is accelerated by CheZ, which shortens the lifetime of the signal by accelerating the dephosphorylation of CheY-P back to CheY. The equation for the phosphorylation/dephosphorylation cycle of CheY then reads

$$\frac{dy}{dt} = k_a a(1 - y) - k_z y, \tag{2}$$

where k_a is a constant that determines the maximal rate of CheY phosphorylation by CheA, and k_z is a constant that determines the rate of CheY-P dephosphorylation by CheZ. The dependence of the steady state CheY-P concentration, y_*, on a is thus hyperbolic, $y_* = a/(a + k_z/k_a)$, and hence effectively linear in the range $a \ll k_z/k_a$ (experimentally, k_z/k_a is found to be close to unity, and $a \simeq 1/3$).

The equilibrium probability of the motor being in the CCW state (run mode) is called the CCW bias, and is a function of y:

$$h(y) = (1 + (y/y_0)^H)^{-1} \tag{3}$$

where y_0 is the CheY-P concentration at which the bias is $1/2$, and the parameter H accounts for the steepness of the sigmoidal response [10]. It follows that the ratio of the probabilities for the CW state and the CCW state is $(y/y_0)^H$. The times between switching events have been shown to be distributed exponentially [11], characteristic of a Markovian one-step process. The switching probability per unit time, is therefore determined by the average lifetime of the CW and CCW events, $\langle \tau_{CW} \rangle$ and $\langle \tau_{CCW} \rangle$, respectively, which are related to h by $h(y) = [1 + \langle \tau_{CW} \rangle / \langle \tau_{CCW} \rangle]^{-1}$.

2.2 Allosteric Switches: From Signal Reception to Motor Control

Experimentally, both the receptor-kinase response to chemoeffector ligands, $G(L, m)$, and the motor response to CheY-P ligands, $h(y)$, are found to be steep, indicative of cooperative effects between the binding sites for chemoeffector in the receptor case, and those for CheY-P in the motor case. These binding sites are closely packed—in two-dimensional arrays in the case of receptors, and in a one-dimensional ring, in the case of the flagellar motor. The physical distance between the binding units are thus short enough for direct protein-protein contact. Ising models that treat individual binding units as coupled lattice elements are thus a natural representation for the behavior of these allosteric systems [12].

In these models, individual binding units are treated as two-state systems, which are in equilibrium between a signal ON state and a signal OFF state. Both ON and OFF states can further be ligand bound or unbound, leading to a total of four possible states. In the absence of ligand, there exists a certain free energy difference, f_0, between the ligand-unbound ON and OFF states. The free energy difference between the ligand-bound and ligand-unbound states depends on the ligand concentration, L, which enters logarithmically (in units of $k_B T$) as $\ln(K/L)$, where K is a dissociation constant. Assuming detailed balance, requiring that the ON state and OFF state have different dissociation constants for ligand, K_{on} and K_{off}, is sufficient to ensure ligand binding will affect the ON/OFF equilibrium. The magnitude of this effect is $\ln(K_{on}/K_{off})$. Solving for the probability of being in the ON state obtains $p_{ON} = (1 + e^{f_0 + f_L(L)})^{-1}$, where $f_L(L) = \ln(1 + L/K_{off}) - \ln(1 + L/K_{on})$.

Coupling between neighboring binding sites results in a steeper response in the lattice, whose state is governed by a Hamiltonian with an additional coupling term,

$$H = \sum_i^N \left(\ln(K_{off}/L) l_i + \sigma_i \left(f_0 + \ln(K_{on}/K_{off}) l_i \right) \right) + \sum_{i,j}^N J(\sigma_i - 1/2)(\sigma_j - 1/2) \tag{4}$$

where σ_i is the activity state of the i-th subunit ($\sigma = 0$ when OFF, $\sigma = 1$ when ON), and l_i is the ligand-binding state of the i-th subunit ($l = 0$ when unbound, $l = 1$ when bound), J is the coupling energy between nearest-neighbor sites, N is the total number of subunits and the double summation runs over edges connecting nearest neighbors.

In general, the behavior of such Ising models requires numerical computations, but a limiting case that is more amenable to analytical treatment is one in which coupling between subunits is so strong ($J \to \infty$) that the activity state of the entire N-site lattice can take one of only two values, $\sigma = \{0, 1\}$. This limit, known as the Monod-Wyman-Changeux (MWC) allosteric model in biochemistry, has a much simpler Hamiltonian,

$$H = \sum_{i}^{N} \left[\ln(K_{off}/L) + \sigma \ln(K_{on}/K_{off})\right] l_i + \sigma N f_0, \tag{5}$$

and the system can be solved analytically for most quantities of interest. The partition function is

$$Z = \sum_{\langle \sigma, j \rangle} \exp(-H) = (1 + L/K_{off})^N (1 + e^{-N(f_0 + f_L(L))}) \tag{6}$$

from which the probability of the ON state can be obtained by computing the average of σ,

$$p_{ON} = \langle \sigma \rangle = -\frac{1}{N} \frac{\partial \ln Z}{\partial f_0} = \left[1 + e^{N(f_0 + f_L(L))}\right]^{-1}. \tag{7}$$

In the case of the flagellar motor, the ON and OFF states can be assigned to the CW and CCW rotational states, so that $p_{ON} = 1 - h(y)$.

In the case of the receptor-kinase, the ON and OFF states can be assigned to the active and inactive states of the kinase, so that $p_{ON} = a$. However, as noted in the previous section, receptor-kinase activity is a function not only of the ligand concentration, L, but also the level of receptor modification, m. This can be incorporated in a natural way by letting the ligand-independent free energy, f_0, to depend on the level of methylation, $f_0 = f_m(m)$. For methylation to increase kinase activity, the dependence of f_m on m must be such that $\partial f_m / \partial m < 0$. Fits of the model to experimental data have revealed a linear form for this function,

$$f_m(m) = \alpha(m_0 - m), \tag{8}$$

where α is a constant accounting for the average free-energy change per added methyl group ($\simeq 2k_BT$), and m_0 is an offset methylation level ($\simeq 0.5$) that sets the kinase activity level in the absence of chemoeffector ligands.

2.3 Precise Adaptation

Upon stimulation with a step of the attractant aspartate, or its non-metabolizable analogue, α-methylaspartate, the output of the chemotaxis system (either in terms of swimming behavior, motor rotation, or receptor-kinase activity) exhibits precise adaptation, i.e. restoration of the output to the pre-stimulus level. A particularly simple condition for ensuring such precision of adaptation was identified in [13]. Specifically, they found that if the rates of the negative feedback reactions, mediated by CheR and CheB, could be made to depend only on the current kinase activity, a, and not on the number of available methylation sites, the property of precise adaptation could be made robust to variations in many parameters of the system, such as the concentration of protein components. We shall see below how this is

accomplished through methylation assistance neighborhoods. Within the scheme discussed above, this implies that the net rate of change of methylation depends only on a, i.e.

$$\frac{dm}{dt} = F(a). \tag{9}$$

Precise adaptation is guaranteed if the system has only a single, globally stable fixed point (at $a = a_0$). Given the monotonic, positive dependence of a on m ($\partial a/\partial m > 0$ for all m), this implies that $F(a)$ crosses zero only once with a negative slope ($F'(a_0) < 0$).

2.4 Assistance Neighborhoods

The independence of methylation rate on the methylation level breaks down when the number of unoccupied methylation sites is small. Given that there are four methylation sites per receptor, adaptation would occur on a quite limited interval of concentrations, much smaller than the one actually observed. The wide range of precise adaptation is explained by the observation that methyltransferase CheR and methylesterase CheB act on so-called "assistance neighborhoods" of 7 and 5 receptor dimers, respectively [14, 17], thus considerably enlarging the number of available modification sites.

A convenient expression for the methylation rate that accounts for the loss of adaptation and the assistance neighborhoods is

$$F(a, m) = k_r[\mathrm{CheR}](1 - a)\frac{M - m}{M - m + K_R} - k_b[\mathrm{CheB}]a\frac{m}{m + K_B} \tag{10}$$

where the mean methylation level per receptor monomer lies in the range $0 \leq m \leq M = 4$. Adaptation is perfect in the limit $K_R, K_B \to 0$. We will see how precise adaptation emerges from the requirement of uptake optimization in fluctuating environments 5.2.

3 Chemotactic Responses to Simple Stimuli

3.1 Summary of the Model

As discussed in the previous sections, the chemotactic transduction pathway can be conveniently modeled by the following set of mean-field equations [6, 15–21]

$$\begin{aligned} a &= G(m, L), \\ \frac{dm}{dt} &= F(a, m), \\ \frac{dy}{dt} &= k_a a(1 - y) - k_z y, \\ \frac{dp_r}{dt} &= \frac{1 - (p_r/h(y))}{\tau_t}. \end{aligned} \tag{11}$$

The detailed expressions for the functions that appear above are

$$\begin{aligned} G(m,L) &= (1+e^{f(m,L)})^{-1}, \\ f(m,L) &= n_a\alpha_m(m_0-m)+n_a\ln\frac{1+L/K_{off}}{1+L/K_{on}}, \\ F(a,m) &= k_r[\mathrm{CheR}](1-a)\frac{M-m}{M-m+K_R}-k_b[\mathrm{CheB}]a\frac{m}{m+K_B}, \\ h(y) &= [1+(y/y_0)^H]^{-1}. \end{aligned} \tag{12}$$

The number of Tar (methyl-)aspartate receptors in a cluster is n_a. The low affinity binding of methyl-aspartate to Tsr (serine receptors) is not included for simplicity. It can be easily added to the free energy, though. The linear dependence of the methylation-dependent part of the free energy has been recently documented in [7].

The recommended values for the parameters are $\alpha_m = 2$, $m_0 = 0.5$, $M = 4$, $K^s_{off} = 2.5$ μM, $K^s_{on} = 1$ mM, $K^a_{off} = 18$ μM, $K^a_{on} = 3$ mM, $k_z = 2$ s^{-1}, $k_a = 3$ s^{-1}, $y_0 = 0.4$, $H = 10$, $[\mathrm{CheR}] = 0.16$ μM, $[\mathrm{CheB}] = 0.28$ μM, $k_r[\mathrm{CheR}] = 0.1$ s^{-1} and $k_b[\mathrm{CheB}] = 0.2$ s^{-1}, $K_R = 0.02$, $K_B = 0.02$. Slightly more refined models account for the phosphorylation of CheB by CheA-P, through the equilibrium expression $[\mathrm{CheB}] = [\mathrm{CheB}]_{tot}a/(a+K_a)$. However, significant deviations from a linear dependence of the methylation rate on the activity are detectable only for large values of the activity (larger than ∼0.7, [7]) characteristic of extremely tumble motion.

3.2 Equilibrium in a Uniform and Stationary Attractant Distribution

In the presence of a uniform distribution of chemoattractant, the average duration of runs can be obtained by looking at the stationary solutions of the model equations, denoted by a star in the following. The resulting equilibrium values are

$$\begin{aligned} \tau_{r,*} &= \tau_t\frac{p_{r,*}}{1-p_{r,*}}, \\ p_{r,*} &= h(y_*), \\ y_* &= \frac{k_a a_*}{k_a a_* + k_z}, \\ a_* &= \frac{1}{1+\frac{k_b[\mathrm{CheB}]m_*(M-m_*+K_R)}{k_r[\mathrm{CheR}](m_*+K_B)(M-m_*)}}, \\ e^{n_a\alpha_m(m*-m_0)}&\frac{k_b[\mathrm{CheB}]m_*(M-m_*+K_R)}{k_r[\mathrm{CheR}](m_*+K_B)(M-m_*)} = \left(\frac{1+L/K^a_{off}}{1+L/K^a_{on}}\right)^{n_a}. \end{aligned} \tag{13}$$

The last equation is transcendental and has to be solved numerically for the methylation level as a function of attractant concentrations. Since the left hand size is an increasing function of m_*, the search is trivial. Direct substitution of the equilibrium value for methylation in (13) yields the average run duration, or the run probability, for given values of ligand concentration. We remark that perfect adaptation is recovered only in the limit when both K_R and K_B vanish and in that case an explicit analytical dependence of methylation on attractant concentration can be derived. The departure from perfect adaptation in response to a small step change is obviously $\Delta\tau_r = (\partial\tau_{r,*}/\partial L)\Delta L$.

3.3 The Chemotactic Response Function

In the linear response regime, any change in concentration can be decomposed as the superposition of responses to elementary stimuli. Therefore, it is sufficient to focus the attention on the response to impulsive changes in concentration.

For mild variations of chemoattractant concentration around a uniform level, i.e. in the linear response limit, the evolution of the running probability takes the customary form of a two-state inhomogeneous Poisson process

$$\frac{dp_r}{dt} = \frac{1}{\tau_t}(1 - p_r) - \frac{1}{\tau_t(\frac{h}{1-h})} p_r. \tag{14}$$

Then, developing to first order around the equilibrium value one obtains

$$\frac{dp_r}{dt} = \frac{1}{\tau_t}(1 - p_r) - \frac{1}{\tau_{r,*}}\left(1 - \frac{h'_* \Delta y}{h_*(1-h_*)}\right) p_r \tag{15}$$

of the rate of conversion from run to tumble when the bacterium is exposed to a variable concentration then reads

$$Q(t) \equiv \frac{h'_* \Delta y(t)}{h_*(1-h_*)} = \int_{-\infty}^{t} K(t-t')L(t')dt' \tag{16}$$

whereby we have introduced the linear response function $K(t)$ to an impulsive change in attractant.

The explicit form of this response function is obtained by integrating the linearized dynamical equations

$$\begin{aligned}
\frac{d\Delta p_r}{dt} &= -\frac{\Delta p_r}{\tilde{\tau}} + \frac{1}{\tau_t}\frac{h'(y_*)}{h(y_*)}\Delta y, \\
\frac{d\Delta y}{dt} &= k_a(1-y_*)\left(\frac{\partial G}{\partial m}\right)_* \Delta m - \frac{\Delta y}{\tau_y}, \\
\frac{d\Delta m}{dt} &= -\frac{\Delta m}{\tau_m},
\end{aligned} \tag{17}$$

where $\tilde{\tau}^{-1} = \tau_t^{-1} + \tau_{r,*}^{-1}$, $\tau_y^{-1} = k_z + k_a a_*$ and $\tau_m^{-1} = -(\frac{\partial F}{\partial a}\frac{\partial G}{\partial m} + \frac{\partial F}{\partial m})_*$.

Equations (17) are supplemented by the initial conditions

$$\begin{aligned}
\Delta m(0) &= \left(\frac{\partial F}{\partial a}\frac{\partial G}{\partial L}\right)_* \Delta L, \\
\Delta y(0) &= k_a(1-y_*)\left(\frac{\partial G}{\partial L}\right)_* \Delta L, \\
\Delta p_r(0) &= 0
\end{aligned} \tag{18}$$

that correspond to an impulsive stimulus $\Delta L\delta(t)$, where $\delta(t)$ is the Dirac delta function. The explicit expressions for the various partial derivatives appearing in the previous formulae

are

$$\begin{aligned}
\left(\frac{\partial F}{\partial a}\right)_* &= -k_r[\mathrm{CheR}]\frac{M-m_*}{M-m_*+K_R} - k_b[\mathrm{CheB}]\frac{m_*}{m_*+K_B} < 0,\\
\left(\frac{\partial F}{\partial m}\right)_* &= -(1-a_*)k_r[\mathrm{CheR}]\frac{K_R}{(M-m_*+K_R)^2} - a_*k_b[\mathrm{CheB}]\frac{K_B}{(m_*+K_B)^2} \le 0,\\
\left(\frac{\partial G}{\partial m}\right)_* &= a_*(1-a_*)\alpha n_a > 0,\\
\left(\frac{\partial G}{\partial L}\right)_* &= -a_*(1-a_*)n_a\frac{(K^a_{off})^{-1}-(K^a_{on})^{-1}}{(1+L/K^a_{off})(1+L/K^a_{on})} < 0.
\end{aligned} \tag{19}$$

The solution reads

$$\begin{aligned}
\Delta m(t) &= \Delta m(0)e^{-t/\tau_m},\\
\Delta y(t) &= \Delta y(0)e^{-t/\tau_y} + k_a(1-y_*)\left(\frac{\partial G}{\partial m}\right)_*\Delta m(0)\frac{e^{-t/\tau_m}-e^{-t/\tau_y}}{\tau_y^{-1}-\tau_m^{-1}},\\
\Delta p_r(t) &= \frac{1}{\tau_t}\frac{h'(y_*)}{h(y_*)}\Bigg[\Delta y(0)\left(\frac{e^{-t/\tau_y}-e^{-t/\tilde{\tau}}}{\tilde{\tau}^{-1}-\tau_y^{-1}}\right) + k_a(1-y_*)\left(\frac{\partial G}{\partial m}\right)_*\Delta m(0)\\
&\quad\times\left(\frac{e^{-t/\tau_y}}{(\tau_y^{-1}-\tau_m^{-1})(\tau_y^{-1}-\tilde{\tau}^{-1})} + \frac{e^{-t/\tau_m}}{(\tau_m^{-1}-\tau_y^{-1})(\tau_m^{-1}-\tilde{\tau}^{-1})}\right.\\
&\quad\left.+\frac{e^{-t/\tilde{\tau}}}{(\tilde{\tau}^{-1}-\tau_y^{-1})(\tilde{\tau}^{-1}-\tau_m^{-1})}\right)\Bigg]
\end{aligned} \tag{20}$$

whence the result for the response to an impulsive stimulus

$$\begin{aligned}
K(t) &= k_a\frac{h'(y_*)(1-y_*)}{h(y_*)(1-h(y_*))}\left(\frac{\partial G}{\partial L}\right)_*\left(\tau_y^{-1}-\tau_m^{-1}\right)^{-1}\\
&\quad\times\left[\left(\tau_y^{-1}e^{-t/\tau_y}-\tau_m^{-1}e^{-t/\tau_m}\right) - \left(\frac{\partial F}{\partial m}\right)_*\left(e^{-t/\tau_m}-e^{-t/\tau_y}\right)\right].
\end{aligned} \tag{21}$$

The response (21) is decomposed in two contributions: the first term inside the square bracket integrates to zero, whereas the second one, proportional to $\partial F/\partial m$, is equal to zero at the time of impulsive stimulation. Notice that right after the stimulation, the response is always positive

$$K(0) = k_a\frac{h'(y_*)(1-y_*)}{h(y_*)(1-h(y_*))}\left(\frac{\partial G}{\partial L}\right)_* > 0. \tag{22}$$

In (21) only the second term inside the square bracket contributes to the full integral and vanishes as expected in case of perfect adaptation:

$$\int_0^\infty K(t)dt = -k_a\tau_y\tau_m\left(\frac{\partial F}{\partial m}\right)_*\frac{h'(y_*)(1-y_*)}{h(y_*)(1-h(y_*))}\left(\frac{\partial G}{\partial L}\right)_* \ge 0. \tag{23}$$

The positive sign of the integral implies that only perfect or partial adaptation can be achieved in this model. Overadaptation is ruled out because: (i) the methylation rate decreases with increasing occupation of methylation sites ($\partial F/\partial m \le 0$); (ii) the activity decreases with ligand concentration ($\partial G/\partial L < 0$); (iii) the counterclockwise frequency decreases with the level of CheY-P and therefore with the activity ($h'(y) < 0$).

In the case of perfect adaptation both τ_y and τ_m do not depend on the mean ligand concentration. Remarkably, for the methylation rate $\tau_m^{-1} = (\partial F/\partial a)(\partial G/\partial m)$ to be independent of L, $\partial G/\partial m$ must be independent of m. Therefore, a linear dependence of the free energy on the methylation level is a necessary condition to obtain a methylation time independent of the attractant level.

For purpose of comparison with previous analyses of the response function, namely [22], it is useful to introduce a "bias response function" defined as the variation in the running frequency $K_b(t) \equiv \Delta p_r(t)/\Delta L$ that follows an impulsive stimulation.

For this response the model gives

$$K_b(t) = \frac{\Delta p_r(t)}{\Delta L} = \frac{1}{\tau_t}\frac{h'(y_*)}{h(y_*)} k_a (1-y_*)\left(\frac{\partial G}{\partial L}\right)_* \left\{ \frac{e^{-t/\tau_y} - e^{-t/\tilde{\tau}}}{\tilde{\tau}^{-1} - \tau_y^{-1}} - \left[\frac{1}{\tau_m} + \left(\frac{\partial F}{\partial m}\right)_*\right] \times \left(\frac{e^{-t/\tau_y}}{(\tau_y^{-1} - \tau_m^{-1})(\tau_y^{-1} - \tilde{\tau}^{-1})} + \frac{e^{-t/\tau_m}}{(\tau_m^{-1} - \tau_y^{-1})(\tau_m^{-1} - \tilde{\tau}^{-1})} + \frac{e^{-t/\tilde{\tau}}}{(\tilde{\tau}^{-1} - \tau_y^{-1})(\tilde{\tau}^{-1} - \tau_m^{-1})} \right) \right\}. \tag{24}$$

This quantity is indeed the bias response measured by the tethering assay in [22], and evaluates to zero at the time of stimulation.

Notice that the integral of the bias response function

$$\int_0^\infty K_b(t)dt = -k_a \tau_y h'(y_*)(1-y_*)\left(\frac{\partial G}{\partial L}\right)_* \left(\frac{\partial F}{\partial m}\right)_* = \frac{\partial p_{r,*}}{\partial L}, \tag{25}$$

is proportional to $\partial F/\partial m$ and equals the derivative of the stationary run probability with respect to the uniform concentration. As expected, it vanishes in the case of perfect adaptation whereas in general $\partial p_{r,*}/\partial L \geq 0$. A similar result holds for the dependence of the average run time, since it is an increasing function of p_r. Again, this reiterates that only perfect or partial adaptation can be achieved.

The straightforward relationship between the two response functions defined above is

$$K_b(t) = \frac{1-h_*}{\tau_t}\int_0^t K(t')e^{-(t-t')/\tilde{\tau}}dt'. \tag{26}$$

The difference resides in the delay $\tilde{\tau}_t$ required to equilibrate the state of motion in response to a change in the motor configuration. In the limit $\tau_t \ll \tau_r$ the two responses coincide to within an overall multiplicative factor τ_t/τ_r, for times larger than τ_t. However, in tethering experiments the measured ratio is roughly 0.6, most likely because of the presence of a single flagellum, and the bias response may differ from $K(t)$ at times smaller than the average tumbling time, circa 0.4 s in that case (see below).

We notice in passing that the methylation time in the linear response regime measured by means of FRET [7] appears to be significantly larger than the value obtained through the bias response [22]. The reasons for this difference are unknown yet.

4 From Microscopic to Macroscopic

4.1 Relating Motility Coefficients and the Linear Response Function

A useful relationship between the microscopic response function and macroscopic behavioral properties of the bacteria can be given in terms of motility coefficients that describe the

dependence of drift and diffusion on the ambient concentration field. As detailed in [8], the motion of a single bacterium (at scales larger than the length of a single run and for smooth, mild spatiotemporal changes in the attractant profile) can be effectively described by the sum of a drift velocity in the direction of the attractant gradient $v = \chi \nabla c$, where χ is the *chemotactic coefficient*, and a diffusion process with coefficient $D = D_0(1 + \gamma c)$ where $D_0\gamma$, the *chemokinetic coefficient*, has the same dimensions as χ [length^2/(time $\cdot$ concentration)]. We remark in passing that this particular type of chemokinesis does not rely upon a variation of the bacterial speed with concentration. Rather, the increase in diffusion is due to the extension of the run time with increasing chemoattractant. The above coefficients are related to the response function introduced above, and the relationship takes a particularly simple form when the tumbling time is negligible with respect to the average run time. The results, obtained by means of a multiple-scale asymptotic analysis, are

$$\chi = D_0 \frac{\alpha}{\sigma} \int_0^\infty e^{-\sigma t} K(t) dt, \tag{27}$$

$$\gamma = \frac{\alpha}{\sigma} \int_0^\infty K(t) dt, \tag{28}$$

$$D_0 = \frac{u^2}{d\sigma}, \qquad \alpha = \frac{1 - \langle \cos\varphi \rangle}{\tau_r}, \qquad \sigma = (d-1) D_{rot} + \alpha \tag{29}$$

where D_{rot} is the rotational diffusivity, u is the speed of the bacterium, φ is the tumbling angle and d is the spatial dimension. It is important to notice that the increase of the diffusion coefficient in response to a uniform concentration of a chemical substance is proportional to the integral of the response function and therefore inversely proportional to the precision of adaptation.

Upon substitution of the explicit expression (21) for the response function, one obtains (omitting the subscripts $_*$ for the ease of notation)

$$\chi = D_0 \frac{\alpha}{\sigma} k_a \frac{h'(y)(1-y)}{h(y)(1-h(y))} \left(\frac{\partial G}{\partial L} \right) \left[\sigma - \left(\frac{\partial F}{\partial m} \right) \right] \left(\sigma + \tau_y^{-1} \right)^{-1} \left(\sigma + \tau_m^{-1} \right)^{-1} > 0, \tag{30}$$

$$\gamma = -\frac{\alpha}{\sigma} k_a \frac{h'(y)(1-y)}{h(y)(1-h(y))} \left(\frac{\partial G}{\partial L} \right) \left(\frac{\partial F}{\partial m} \right) \tau_y \tau_m \geq 0. \tag{31}$$

These results hold whenever the lengthscale of variation of the concentration field is much larger than the typical run length, $L/(\partial L/\partial x) \gg u\tau_r$. This is not a severe limitation as it is empirically found that scale separations of order 3 or 4 are often sufficient to ensure the validity of the expressions obtained by means of homogenization techniques. An additional condition is that the timescale of variation of the chemoattractant along the bacterial trajectory should be slow with respect to both the run time and the response timescale (i.e. the rate of exponential decay of $K(t)$). In the following sections we lift the latter requirement, in order to allow for fast changes in the chemoattractant profile. We start by giving a heuristic derivation of the effective transport equation for the bacterial probability density, deferring the derivation by homogenization techniques to the Appendix.

4.2 Heuristic Derivation of the Macroscopic Equations

The orientation of the bacterium $\hat{u}(t)$ evolves over a short time Δt according to the following Markov process

$$\hat{u}(t+\Delta t) = \begin{cases} R_T \hat{u}(t) & \text{w.p. } \frac{\Delta t}{\tau_r}(1-Q(t))p(t,\hat{u}(t)), \\ R_D(\Delta t)\hat{u}(t) & \text{w.p. } 1-\frac{\Delta t}{\tau_r}(1-Q(t))p(t,\hat{u}(t)), \end{cases} \tag{32}$$

where $p(t,\hat{u}(t))$ is the probability of observing the orientation $\hat{u}(t)$ at time t and w.p. stands for "with probability". R_T and $R_D(\Delta t)$ are rotation matrices that perform the change in orientation due to tumbling and rotational diffusion with coefficient D_{rot}, respectively. The modulation of the rate of transition from run to tumble is

$$Q(t) = \int_{-\infty}^{t} K(t-s)c(X(s),s)ds \tag{33}$$

where $X(s)$ is the position of the bacterium in space, and c is the concentration of ligand (previously denoted by L). The modulus of the velocity field is constant and equal to u.

Drift in a Variable Gradient The average vector velocity obeys

$$\begin{aligned} \langle \overline{u}(t+\Delta t)\rangle = &\left(1-\frac{\Delta t}{\tau_r}\right)\langle R_D(\Delta t)\rangle \langle \overline{u}(t)\rangle + \frac{\Delta t}{\tau_r}\langle R_T\rangle \langle \overline{u}(t)\rangle \\ &+ \frac{\Delta t}{\tau_r}\left(\langle R_D(\Delta t)\rangle - \langle R_T\rangle\right)\langle \overline{u}(t)Q(t)\rangle . \end{aligned} \tag{34}$$

The averages of the rotation matrices are easily evaluated: $\langle R_T\rangle = \langle\cos\varphi\rangle I$ and $\langle R_D(\Delta t)\rangle = [1 - D_{rot}(d-1)\Delta t]I$ where I stands for the identity matrix. In the absence of chemoattractant, $Q = 0$, the exact solution for the average velocity is therefore $\langle \overline{u}(t)\rangle = \overline{u}(0)\exp[-(D_{rot}(d-1) + (1-\langle\cos\varphi\rangle)/\tau_r)t]$ in d spatial dimensions. This result yields the time-correlation matrix

$$\begin{aligned} \langle \overline{u}(t)\otimes\overline{u}(0)\rangle_{Q=0} &= I\frac{u^2}{d}\exp[-(D_{rot}(d-1) + (1-\langle\cos\varphi\rangle)\tau_r^{-1})t] \\ &= I\frac{u^2}{d}\exp(-\sigma t), \end{aligned} \tag{35}$$

where we have made use of the identity $\langle \overline{u}(0)\otimes\overline{u}(0)\rangle_{Q=0} = \frac{I}{d}$. In the presence of chemoattractant, the stationary drift is

$$\langle \overline{u}(t)\rangle_r = \frac{1-\langle\cos\varphi\rangle}{1-\langle\cos\varphi\rangle + D_{rot}\tau_r(d-1)}\langle \overline{u}(t)Q(t)\rangle = \frac{\alpha}{\sigma}\langle \overline{u}(t)Q(t)\rangle , \tag{36}$$

where α and σ have been defined in the previous section. The final step is to express the modulation as a history term over the previous values of the velocity. Only two assumptions are required to complete the calculation of the mean velocity and therefore of the chemotactic coefficient.

First, we shall assume that the variation in concentration is small enough to warrant that the modulation be small, $|Q| \ll 1$. Second, we require that the spatial scale of variation of

the concentration be slow with respect to the typical length of a single run. In this case one has the linear expansion

$$c(X(s),s) \simeq c_0(s) + g(s)(X(s) - x_0) = c_0(s) - g(s)x_0 + g(s)\int_{-\infty}^{s} \overline{u}(s')ds', \qquad (37)$$

where g is the local gradient of concentration. Plugging the latter expression into the definition of Q, (33), and evaluating the averages at $Q = 0$ gives

$$\begin{aligned}\langle \overline{u}(t)Q(t)\rangle &\simeq \int_{-\infty}^{t} ds g(s)K(t-s)\int_{-\infty}^{s} ds' \left\langle \overline{u}(t)\otimes\overline{u}(s')\right\rangle_0 \\ &= \frac{u^2}{d\sigma}\int_{-\infty}^{t} g(s)\exp[-\sigma(t-s)]K(t-s)ds, \end{aligned} \qquad (38)$$

where we have made use of $\langle \overline{u}(t)\rangle_{Q=0} = 0$. The exponential cutoff on the fast time-scale σ^{-1} is the loss of memory of the past trajectory due to rotational diffusion and tumbling. This leads to the final expression for the drift velocity and the chemotactic coefficient

$$v(x,t) = D_0\frac{\alpha}{\sigma}\int_{-\infty}^{t} e^{-\sigma(t-s)}K(t-s)\nabla c(x,s)ds, \qquad (39)$$

that coincides with the expression derived in [8] in the limit of gradients that vary slowly with respect to the longest response time.

Effective Diffusion The calculation of the chemokinetic contribution is performed by considering a uniform, time-dependent concentration field, and makes use of the Taylor-Green-Kubo formula that expresses the effective diffusion coefficient through the velocity time autocorrelation:

$$\begin{aligned} D_{\mathit{eff}} &= d^{-1}\int_0^{\infty} \langle \overline{u}(t)\cdot\overline{u}(0)\rangle\, dt \\ &= u^2 d^{-1}\int_0^{\infty} \exp\left(-(\sigma - \alpha Q)t\right) dt \simeq \frac{u^2}{d\sigma}\left(1 + \frac{\alpha}{\sigma}Q(t)\right). \end{aligned} \qquad (40)$$

In the derivation of this result we have exploited the time separation between the decay of the velocity autocorrelation, that takes place on a fast timescale of the order of τ_r, and the variation of $Q(t)$ that occurs on slower timescales. The latter are of the order of the correlation time of c, or of the order of the slowest response time, whichever the longest.

The resulting effective diffusion coefficient reads

$$D_{\mathit{eff}}(x,t) = D_0\left(1 + \frac{\alpha}{\sigma}\int_{-\infty}^{t} K(t-s)c(x,s)ds\right), \qquad (41)$$

which again coincides with the results of [8] for concentrations varying more slowly than the response time.

Transport Equation Summarizing, the evolution of the bacterial number density in an environment with a variable distribution of chemoattractant obeys the Fokker Planck equation

$$\frac{\partial n(x,t)}{\partial t} + \nabla(v(x,t)n(x,t)) = \nabla^2\left(D_{\mathit{eff}}(x,t)n(x,t)\right) \qquad (42)$$

with drift and diffusion coefficients as in (39) and (41), respectively. We recall that the assumptions required to derive this result are: the response is linear and small ($Q \ll 1$); the gradients change smoothly in space.

5 Functional Aspects of the Chemotaxis Response

In order to assess whether or not a given response is advantageous, it is necessary to evaluate its evolutionary performance, namely its fitness. In order to keep the discussion general, we shall assume that the fitness is a generic function monotonically increasing with the chemoattractant uptake rate R. The latter is in turn proportional to the local concentration in the diffusion-limited case. While it is known that some chemoattractants are not directly metabolized, they are likely to serve as proxy for beneficial orientations so that the assumption of fitness monotonicity seems quite sensible.

The uptake rate R then reads

$$\begin{aligned} R &= J \int dx c(x,t) n(x,t) = R_0 + R' \\ &= J \int dx c(x,t) \left\{ n_0 + \int_{-\infty}^{t} ds \left[-\nabla \left(v(x,s) n(x,s) \right) + \nabla^2 \left(D_{eff}(x,s) n(x,s) \right) \right] \right\}, \end{aligned} \tag{43}$$

where n_0 denotes the initial, uniform in space distribution of bacteria and the proportionality constant J is itself proportional to the diffusion-limited rate of attractant to the cell surface (units of volume/time, e.g. $4\pi D_c a$ for a sphere of radius a).

At the lowest orders in chemoattractant concentration, the two terms featuring in the uptake rate are

$$\begin{aligned} R_0 &= J n_0 \int dx c(x,t), \\ R' &= J n_0 \frac{D_0 \alpha}{\sigma} \int dx \int_{-\infty}^{t} ds \int_{-\infty}^{s} ds' K(s-s') \\ &\quad \times \left(e^{-\sigma(s-s')} \nabla c(x,s') \nabla c(x,t) + c(x,s') \nabla^2 c(x,t) \right). \end{aligned} \tag{44}$$

The first one is the "bare" uptake rate (the one obtained in absence of any response) and the second one, quadratic in c, is the actual gain due to chemotactic motion.

When the response time is faster than the correlation time of the chemoattractant field, $\tau_y^{-1}, \tau_m^{-1} \gg \partial_t c / c$, the gain reads

$$R' = J n_0 \left[\chi \int dx (\nabla c(x,t))^2 + D_0 \gamma \int dx c(x,t) \nabla^2 c(x,t) \right]. \tag{45}$$

For a linear, static gradient, one has $R' = J n_0 \chi (\nabla c)^2$ and the best response is the one that maximizes χ. This implies that the optimal response function in a gradient is just positive and therefore non-adaptive, as first suggested De Gennes in [24]. Why does adaptation emerge, then? The answer to this question requires a major shift of perspective. Indeed, rather than asking for the optimal response in a given environment, one has to seek for the best response in the worst possible conditions. This risk-minimizing strategy, dubbed MaxiMin in the game-theoretical context, is realized by imposing $\gamma = 0$ and $\chi > 0$. Indeed, this warrants a positive gain for *all* chemoattractant fields. Maximization of R' under the

perfect adaptation condition $\gamma = 0$ leads to a predicted bias response function that compares very well with experimental measurements [8]. This agreement suggests that the chemotactic response has been shaped in hostile, fluctuating environments. In summary, *E. coli* is a realist that tries to do its best in the worst possible conditions, which are those where chemotaxis is most necessary and selected.

5.1 Chemotaxis in Random, Statistically Homogeneous Environments

From now on we will focus on a random concentration field c, statistically homogeneous in space and statistically stationary in time. A priori, this class of environments has a potential for exploitation, since it does not represent the worst possible case. However, for short correlation times it effectively models an unpredictable environment and we shall show how the MaxiMin emerges in those conditions.

The gain in uptake rate, averaged over the ensemble of concentrations is

$$\langle R' \rangle = N_0 \frac{D_0 \alpha}{\sigma} \int_{-\infty}^{t} ds \int_{-\infty}^{s} ds' K(s-s') \left(e^{-\sigma(s-s')} - 1 \right) \langle \nabla c(x,s') \cdot \nabla c(x,t) \rangle, \quad (46)$$

where we have made use of the statistical invariance under spatial translations and N_0 is the total number of bacteria inside the volume of interest. In order to make further progress one has to specify a form for the time-correlation function of the chemoattractant. We shall adopt the expression ($s' < t$)

$$\langle \nabla c(x,s') \cdot \nabla c(x,t) \rangle = \langle |\nabla c|^2 \rangle e^{-(t-s')/\tau_c} \quad (47)$$

that encompasses a large number of situations of interest including, for instance, the diffusion/degradation equation in presence of random sources uncorrelated in time and space. Adopting the generic expression for the linear response function

$$K(t) = \sum_k A_k e^{-\lambda_k t} \quad (48)$$

the resulting increase in uptake rate, or chemotactic gain, becomes

$$\langle R' \rangle = -N_0 D_0 \alpha \tau_c \langle |\nabla c|^2 \rangle \sum_k \frac{A_k}{(\lambda_k + \sigma + \tau_c^{-1})(\lambda_k + \tau_c^{-1})}. \quad (49)$$

The latter expression provides the basis for the identification of the response that is best suited to coping with a variable chemoattractant profile.

5.2 The Optimal Response in a Fluctuating Environment

From the response function (21) obtained in the previous section one can identify the parameters

$$\begin{aligned} &\lambda_1 = \tau_y^{-1}, \qquad \lambda_2 = \tau_m^{-1}, \\ &A_1 = k_a \frac{h'(y)(1-y)}{h(y)(1-h(y))} \left(\frac{\partial G}{\partial L} \right) (\tau_y^{-1} - \tau_m^{-1})^{-1} \left(\tau_y^{-1} + \frac{\partial F}{\partial m} \right), \\ &A_2 = -k_a \frac{h'(y)(1-y)}{h(y)(1-h(y))} \left(\frac{\partial G}{\partial L} \right) (\tau_y^{-1} - \tau_m^{-1})^{-1} \left(\tau_m^{-1} + \frac{\partial F}{\partial m} \right) \end{aligned} \quad (50)$$

obtaining the following expression for the gain

$$\begin{aligned}\langle R' \rangle = &-N_0 D_0 \alpha \tau_c \langle |\nabla c|^2 \rangle k_a \frac{h'(y)(1-y)}{h(y)(1-h(y))} \left(\frac{\partial G}{\partial L} \right) \\ &\times \frac{1}{(\tau_y^{-1} - \tau_m^{-1})} \left(\frac{\tau_y^{-1} + \frac{\partial F}{\partial m}}{(\tau_y^{-1} + \sigma + \tau_c^{-1})(\tau_y^{-1} + \tau_c^{-1})} \right. \\ &\left. - \frac{\tau_m^{-1} + \frac{\partial F}{\partial m}}{(\tau_m^{-1} + \sigma + \tau_c^{-1})(\tau_m^{-1} + \tau_c^{-1})} \right), \end{aligned} \tag{51}$$

where all the quantities are evaluated at equilibrium.

Notice that for very short correlation times $\tau_c^{-1} \gg \tau_m^{-1}, \tau_y^{-1}, \sigma$, the gain is always negative: chemotaxis is advantageous only if the response times and the run time are faster than, or comparable with, the correlation time.

The maximization of the chemotactic gain involves the following independent biochemical parameters: k_r[CheR], k_b[CheB], K_R, K_B, k_z, k_a. We shall not perform the optimization over the parameters describing the sensitivity of the receptor cluster and the steepness of the motor response. These values are likely to be set by a balance between signal amplification and noise, which is not considered in the present work.

The Functional Value of Adaptation It proves convenient to use a different, yet equivalent set of parameters: τ_m^{-1}, τ_y^{-1}, $\partial F/\partial m$, y, a (linked to the previous ones by the equilibrium conditions, e.g. $k_z = (1-y)\tau_y^{-1}$, $k_a = ya^{-1}\tau_y^{-1}$ and by the definitions of τ_m^{-1} and $\partial F/\partial m$). Let us then consider the optimization with respect to $\partial F/\partial m$. The linear dependence of the gain on $\partial F/\partial m$ implies that the maximum is attained at the boundary of the domain of variation of this argument. Since the factor that multiplies $\partial F/\partial m$ in $\langle R' \rangle$ is always positive whereas $\partial F/\partial m \leq 0$, the best response must satisfy $\partial F/\partial m = 0$. In terms of the original parameters, this requires $K_B = K_R = 0$. Therefore, perfect adaptation emerges as the optimal strategy to cope with fluctuating environments.

The Optimal Response Function It is important to recall that our results hold in the limit of small, linear response. If optimization is performed without any constraints it leads to infinite values for the kinetic rates, infinite gain and a contradiction with the assumptions made in deriving the previous formula for the gain. In order to maintain the self-consistency of our approach, we have searched the maximum gain over the space of variables k_r[CheR], k_b[CheB], K_R, K_B, k_z, while keeping a fixed value of k_a. The resulting gain is an increasing function of k_a. The latter value is set to the largest one that warrants a small, linear response (specifically for $\langle Q^2 \rangle^{1/2} < 0.2$ this is obtained for $k_a \simeq 3\ \mathrm{s}^{-1}$). The full problem of optimization *ab initio* requires a fully nonlinear treatment that precludes most, if not all, analytical approaches and is not discussed here. The results of the numerical maximization of the gain function are summarized in Fig. 2. The maximum relative gain is achieved at the concentration where the relative response in activity $\partial G/\partial L/L$ is maximal. The increase in gain for longer correlation times shows that such environments are better exploitable than short-correlated ones. The optimal responses are adaptive in the whole range of correlation times and ligand concentrations that we have investigated. However, environments with a long correlation time are best dealt with a slower response function. Longer τ_c imply slower methylation rates and, to a much lesser extent, slower dephosphorylation times. When the correlation time is $\tau_c \simeq 3$ s, the optimal response shows an activity level $a \approx 1/3$, a CheY phosphorylation fraction $y \approx 0.35$, an average run time $\tau_r \approx 1$ s, $\tau_y \approx 0.3$ s and $\tau_m \approx 1$ s, in

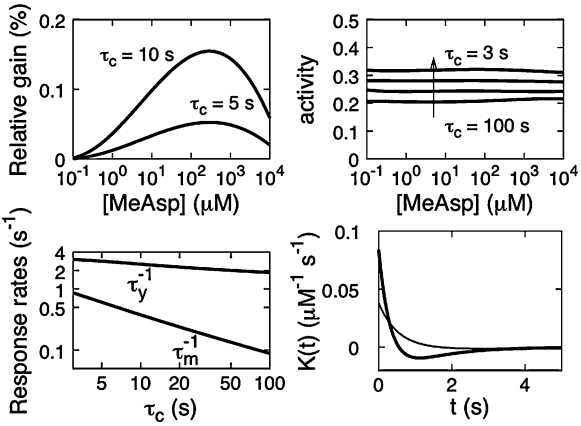

Fig. 2 The optimal response to fluctuating concentration. *Top-left*: the optimal relative gain $\langle R' \rangle / \langle R_0 \rangle$ as a function of methyl-aspartate concentration for two different correlation times. Here a gradient $\nabla c/c = 10^{-3}\ \mu\text{m}^{-1}$ is considered. The rotational diffusivity is $D_{rot} = 0.05\ \text{rad}^2/\text{s}$. *Top-right*: the activity of the optimal response is independent of the ligand concentration. For short-correlated chemoattractant fields, the optimal activity tends to a value $\simeq 1/3$. *Bottom-left*: optimal methylation and dephosphorylation times appearing in the response function. At short correlation times the two timescales tend to be comparable. At $\tau_c = 3$ s, one has $\tau_y \approx 0.3$ s and $\tau_m \approx 1$ s. *Bottom-right*: Optimal linear response function. Short-correlated concentration fields induce adaptation on fast timescales with a characteristic two-lobe response

very good agreement with the numerical values obtained in the previous modeling literature and previously listed. In summary, the observed response function appears to have been selected to provide an optimal gain in uptake rate when facing a rapidly changing environment.

6 Conclusions and Discussions

The possibility that a biological processing network adapts to the statistics of the input signal to maximize its performance is an old and appealing idea [25–27]. In the neurosciences, this possibility has received solid and consistent support, e.g. in the processing of visual images [28, 29]. In the context of bacterial chemotaxis, adaptation has hitherto restrictively referred to the background mean concentration. This implicitly amounts to postulating that the environments where chemotaxis is selected feature small and static gradients superimposed upon a background concentration that varies over several orders of magnitude. Quantitative data on *E. coli* environmental conditions is unfortunately not available, yet existing information indicates the following: (i) as already noted in the introduction, the motility of bacteria peaks in well-defined conditions of scarce nutrients; (ii) the amplitude of the chemotactic response to aspartate is experimentally observed to be important for a range of about a couple of decades [30], much smaller than the range where adaptation to the background level of aspartate is observed; (iii) the same feature as in (ii) is observed in theoretical models that were discussed here. Using the expression of the response function derived in the previous sections, it is indeed immediately checked that the amplitude of the response falls off rapidly for concentrations of the ligand outside the range (K_{off}, K_{on}) of receptors' affinities in the OFF and ON states; (iv) important parameters, such as the ratio between the number of receptors for aspartate (Tar) and serine (Tsr), appear to vary over relatively short time scales

[31] pointing at the plasticity of the network. The upshot of the previous points is that the problem of environmental conditions where chemotaxis is selected is wide open as well as the influence that those conditions exert upon the evolutionary paths shaping the chemotaxis network.

Here, we have described recent work that we performed as first steps in these novel directions. First, assaying the response to input signals with a non-trivial temporal structure has permitted to shed light upon the molecular chemotaxis network structure. Controlling the experimental conditions remains a non-trivial challenge, yet microfluidics is making spectacular progress and it is possible to engineer well-controlled environments where the response of bacteria can be assayed quantitatively. One possible application that we foresee is that the response to non-trivial input signals will permit to probe aspects of the dynamics such as receptor clustering. In fact, while data in [32] indicate a better agreement with the allosteric limit, more precise information is needed to rule out Ising-type interactions, especially if models of the clusters are allowed to feature the dynamics seen in recent experiments using photoactivation localization microscopy (PALM), which allows imaging of receptor clusters with single-molecule resolution [33]. Furthermore, PALM methods are poised to allow probing the role of copy-number fluctuations and molecular diffusion in the network dynamics [34].

Second, non-trivial environmental conditions are important beyond their role as probe tools. What we have shown here is that a fluctuating environment can lead to adaptation, which was previously entirely attributed to the extension of the dynamic range to the mean chemoattractant level. Quantitative experiments will definitely be needed to disentangle the contribution of the two mechanisms to the observed adaptation to aspartate (and the reason for its absence in the response to serine [35]). However, already at this stage it is fair to say that the results provide for a striking instance of the role that the environment can play and a stimulus to explore the amount of adaptation of the chemotaxis network to the environmental statistics.

In conclusion, despite of the fact that chemotaxis is by now a classical subject and has witnessed many years of important progress, the field is extremely active and novel directions remain unexplored and extremely promising. The issues discussed here appear particularly appropriate for quantitative studies, providing a fertile ground for research combining biological and physical tools and methods.

Acknowledgements We thank J. Lebowitz for the organization of the 102nd Statistical Mechanics Conference in December 2009 and for the invitation to contribute to this special issue. A.C. and M.V. have been supported by the ANR Contracts PNANO and PiriBio, by C'Nano IdF and by the CNRS "Prise de risques". TSS has been supported by NWO/FOM.

Appendix: Derivation of the Macroscopic Equations by Homogenization Techniques

In this section we derive systematically the transport equation by means of asymptotic, multiple-scale analysis. Let us consider a bacterium endowed with a linear response function $K(t) = \sum_k A_k e^{-\lambda_k t}$. The choice of the specific form of the response function is obviously inspired by the model for *E. coli* described in the previous sections, although it applies in general to any linearization of a dynamically stable signal transduction model, possibly with the inclusion of complex conjugate pairs for the response decay rates λ and polynomial prefactors in case of degeneracy. Along the bacterial trajectory $X(t)$, the biochemical state of the bacterium is fully specified by the values y of a set of "internal variables", defined as

follows

$$y_k(t) = \int_0^t e^{-\lambda_k (t-s)} c(X(s), s) ds \tag{52}$$

and in terms of which the modulation reads $Q = \sum_k A_k y_k$. The introduction of these variables of state allows to describe the bacterial trajectory as a Markov process governed by the Kolmogorov equation for the probability $p(t, x, \hat{u}, y)$ that a bacterium is found at position x at time t, while running in direction $\hat{u}$, and internal state y:

$$\partial_t p + \overline{u} \nabla p + \sum_k \frac{\partial}{\partial y_k} (c - \lambda_k y_k) p = D_{rot} \nabla^2_{\hat{u}} p - \frac{1 - Q}{\tau_r} \left(p - \int W(\hat{u} \cdot \hat{u}') p(\hat{u}') d\hat{u}' \right), \tag{53}$$

where W is the transition probability for a tumbling event from $\hat{u}'$ to $\hat{u}$. Since the interest is in the spatial density, it is necessary to perform the integration over the angular and internal degrees of freedom. The nonlinearity in the term Qp introduces a hierarchical closure problem. However, for small responses it is immediate to truncate the averaged equations by neglecting terms of order $o(Q)$. The ensuing equations are

$$\begin{aligned}
&\partial_t \langle p \rangle + \nabla \langle J \rangle = 0, \\
&\partial_t \langle J \rangle + \frac{u^2}{d} \nabla \langle p \rangle = -\sigma \langle J \rangle + \alpha \langle Q J \rangle, \\
&\partial_t \langle y_k p \rangle + \nabla \langle y_k J \rangle - c \langle p \rangle + \lambda_k \langle y_k p \rangle = 0, \\
&\partial_t \langle y_k J \rangle + \frac{u^2}{d} \nabla \langle y_k p \rangle - c \langle J \rangle + \lambda_k \langle y_k J \rangle = -\sigma \langle y_k J \rangle,
\end{aligned} \tag{54}$$

where $J = \overline{u} p$, α and σ are defined as previously and $\int \hat{u} W(\hat{u} \cdot \hat{u}') d\hat{u} = \langle \cos \varphi \rangle \hat{u}'$.

This set of equations is still too unwieldy to extract useful information, so that further simplification is advisable. In this framework, the homogenization approach seeks an effective description of the dynamics of p at large scales and long times compared with the typical run distance and time.

This is accomplished by introducing a set of slow variables that scale, in the present case, as ϵx and $\epsilon^2 t$ (for further generalities on homogenization techniques, the reader is invited to consult [23]). Here we extend the results obtained in [8], by allowing a dependence of the concentration field on the fast time variable as well, while retaining a dependence on slow space variables only. Developing the probability density in powers of the small quantity ϵ, computing the derivatives according to $\partial_t \to \partial_t + \epsilon^2 \partial_T$, $\partial_x \to \epsilon \partial_x$, and collecting terms to order ϵ^0 one obtains:

$$\begin{aligned}
&\partial_t \left\langle p^{(0)} \right\rangle = 0, \\
&\partial_t \left\langle J^{(0)} \right\rangle = -\sigma \left\langle J^{(0)} \right\rangle + \alpha \left\langle Q J^{(0)} \right\rangle, \\
&\partial_t \left\langle y_k p^{(0)} \right\rangle - c \left\langle p^{(0)} \right\rangle + \lambda_k \left\langle y_k p^{(0)} \right\rangle = 0, \\
&\partial_t \left\langle y_k J^{(0)} \right\rangle - c \left\langle J^{(0)} \right\rangle + \lambda_k \left\langle y_k J^{(0)} \right\rangle = -\sigma \left\langle y_k J^{(0)} \right\rangle.
\end{aligned} \tag{55}$$

The first equation above shows that $p^{(0)}$ does not depend on the fast time variable. The second and the fourth one imply that after a short transient of about τ_r, both the flux $\langle J^{(0)} \rangle$ and its first moments $\langle y_k J^{(0)} \rangle$ decay to zero and therefore may be considered as independent

of the fast time as well. This is not the case for the first moment of the density that carries along a memory of the past chemoattractant concentrations

$$\left\langle y_k p^{(0)}(x,t)\right\rangle = \left[\int_{-\infty}^{t} e^{-\lambda_k (t-s)} c(x,s) ds\right] \left\langle p^{(0)}(x,t)\right\rangle. \tag{56}$$

At order ϵ, the relevant equations are

$$\begin{aligned} &\partial_t \left\langle J^{(1)}\right\rangle + \frac{u^2}{d} \nabla \left\langle p^{(0)}\right\rangle = -\sigma \left\langle J^{(1)}\right\rangle + \alpha \left\langle Q J^{(1)}\right\rangle, \\ &\partial_t \left\langle y_k J^{(1)}\right\rangle + \frac{u^2}{d} \nabla \left\langle y_k p^{(0)}\right\rangle - c \left\langle J^{(1)}\right\rangle + \lambda_k \left\langle y_k J^{(1)}\right\rangle = -\sigma \left\langle y_k J^{(1)}\right\rangle, \end{aligned} \tag{57}$$

that are easily solved by a Laplace transform over (fast) time (denoted by a tilde, with argument r)

$$\begin{aligned} &r\widetilde{\langle J^{(1)}\rangle} + \frac{u^2}{d} \nabla \langle p^{(0)}\rangle = -\sigma \widetilde{\langle J^{(1)}\rangle} + \alpha \widetilde{\langle Q J^{(1)}\rangle}, \\ &r\widetilde{\langle y_k J^{(1)}\rangle} + \frac{u^2}{d} \nabla \widetilde{\langle y_k p^{(0)}\rangle} - \widetilde{\langle c J^{(1)}\rangle} + \lambda_k \widetilde{\langle y_k J^{(1)}\rangle} = -\sigma \widetilde{\langle y_k J^{(1)}\rangle}, \end{aligned} \tag{58}$$

where the tilde does not appear over $p^{(0)}$ since it does not depend on fast variables. From the equation at order ϵ^0 one obtains $\widetilde{\langle y_k p^{(0)}\rangle} = (r+\lambda_k)^{-1} \tilde{c} \langle p^{(0)}\rangle$.

Upon substitution in the previous expression, expansion to lowest order in c, and trivial algebraic manipulations, the Laplace transform of spatial flux of probability reads

$$\begin{aligned} \widetilde{\langle J^{(1)}\rangle} = (r+\sigma)^{-1} \Bigg[& D_0 \alpha \left(\sum_k A_k \left(r+\lambda_k+\sigma\right)^{-1} \nabla \tilde{c} \right) \left\langle p^{(0)}\right\rangle \\ & - D_0 \nabla \left(\left(1 + \frac{\alpha}{\sigma} \sum_k A_k \left(r+\lambda_k\right)^{-1} \tilde{c} \right) \left\langle p^{(0)}\right\rangle \right) \Bigg], \end{aligned} \tag{59}$$

or, in real time, after a short transient of the order of σ^{-1}

$$\begin{aligned} \langle J^{(1)}\rangle = & \left[D_0 \frac{\alpha}{\sigma} \int_{-\infty}^{t} e^{-\sigma(t-s)} K(t-s) \nabla c(s) ds \left\langle p^{(0)}\right\rangle \right] \\ & - \nabla \left[D_0 \left(1 + \frac{\alpha}{\sigma} \int_{-\infty}^{t} K(t-s) c(s) ds \right) \left\langle p^{(0)}\right\rangle \right], \end{aligned} \tag{60}$$

where one recognizes the drift and diffusion terms heuristically derived in the main text:

$$v(x,t) = D_0 \frac{\alpha}{\sigma} \int_{-\infty}^{t} e^{-\sigma(t-s)} K(t-s) \nabla c(x,s) ds \tag{61}$$

and

$$D_{eff}(x,t) = D_0 \left(1 + \frac{\alpha}{\sigma} \int_{-\infty}^{t} K(t-s) c(x,s) ds \right). \tag{62}$$

To conclude, it remains to analyze the equation at order ϵ^2 that gives the dynamics of the bacterial density $\langle p^{(0)}\rangle$ at large scales and slow times

$$\partial_T \langle p^{(0)}\rangle + \nabla (v \langle p^{(0)}\rangle) = \nabla^2 (D_{eff} \langle p^{(0)}\rangle) \tag{63}$$

that coincides with the one derived heuristically.

References

1. Berg, H.C.: *E. coli* in Motion, Springer, New York (2003)
2. Vergassola, M., Villermaux, E., Shraiman, B.I.: Infotaxis: searching without gradients. Nature **445**, 406–409 (2007)
3. Adler, J., Templeton, B.: The effect of environmental conditions of *Escherichia coli*. J. Gen. Microbiol. **46**, 175–184 (1967)
4. Staropoli, F., Alon, U.: Computerized analysis of chemotaxis at different stages of bacterial growth. Biophys. J. **78**, 513–519 (2000)
5. Wei, Y., Wang, X., Liu, J., Nemenman, I., Singh, A.H., Weiss, H., Levin, B.R.: The population dynamics of bacteria in physically structured habitats and the adaptive virtue of random motility. Proc. Natl. Acad. Sci. USA **108**, 4047–4052 (2011)
6. Tu, Y., Shimizu, T.S., Berg, H.C.: Modeling the chemotactic response of *Escherichia coli* to time-varying stimuli. Proc. Natl. Acad. Sci. USA **105**, 14855–14860 (2008)
7. Shimizu, T.S., Tu, Y., Berg, H.C.: A modular gradient-sensing network for chemotaxis in *Escherichia coli* revealed by responses to time-varying stimuli. Mol. Syst. Biol. **6**, 382 (2010)
8. Celani, A., Vergassola, M.: Bacterial strategies for chemotaxis response. Proc. Natl. Acad. Sci. USA **107**, 1391–1396 (2010)
9. Vladimirov, N., Sourjik, V.: Chemotaxis: how bacteria use memory. Biol. Chem. **390**, 1097–1104 (2009)
10. Cluzel, P., Surette, M., Leibler, S.: An ultrasensitive bacterial motor revealed by monitoring signaling proteins in single cells. Science **287**, 1652–1655 (2000)
11. Bai, F., Branch, R.W., Nicolau, D.V., Pilizota Jr., T., Steel, B.C., Maini, P.K., Berry, R.M.: Conformational spread as a mechanism for cooperativity in the bacterial flagellar switch. Science **327**, 685–689 (2010)
12. Bray, D., Duke, T.A.J.: Conformational spread: the propagation of allosteric states in large multiprotein complexes. Annu. Rev. Biophys. Biomol. Struct. **33**, 53–73 (2004)
13. Barkai, N., Leibler, S.: Robustness in simple biochemical networks. Nature **387**, 913–917 (1997)
14. Li, M., Hazelbauer, G.L.: Adaptational assistance in clusters of bacterial chemoreceptors. Mol. Microbiol. **56**, 1617–1626 (2005)
15. Mello, B.A., Tu, Y.: An allosteric model for heterogeneous receptor complexes: understanding bacterial chemotaxis responses to multiple stimuli. Proc. Natl. Acad. Sci. USA **102**, 17354–17359 (2005)
16. Keymer, J.E., Endres, R.G., Skoge, M., Meir, Y., Wingreen, N.S.: Chemosensing in *Escherichia coli*: two regimes of two-state receptors. Proc. Natl. Acad. Sci. USA **103**, 1786–1791 (2006)
17. Hansen, C.H., Endres, R.G., Wingreen, N.S.: Chemotaxis in *Escherichia coli*: a molecular model for robust precise adaptation. PLoS Comput. Biol. **4**, e1 (2008)
18. Vladimirov, N., Løovdok, L., Lebiedz, D., Sourjik, V.: Dependence of bacterial chemotaxis on gradient shape and adaptation rate. PLoS Comput. Biol. **4**, e1000242 (2008)
19. Emonet, T., Cluzel, P.: Relationship between cellular response and behavioral variability in bacterial chemotaxis. Proc. Natl. Acad. Sci. USA **105**, 3304–3309 (2008)
20. Jiang, L., Ouyang, Q., Tu, Y.: A mechanism for precision-sensing via a gradient-sensing pathway: a model of *Escherichia coli* thermotaxis. Biophys. J. **97**, 74–82 (2009)
21. Vladimirov, N., Lebiedz, D., Sourjik, V.: Predicted auxiliary navigation mechanism of peritrichously flagellated chemotactic bacteria. PLoS Comput. Biol. **6**, e1000717 (2010)
22. Segall, J.E., Block, S.M., Berg, H.C.: Temporal comparisons in bacterial chemotaxis. Proc. Natl. Acad. Sci. USA **83**, 8987–8991 (1986)
23. Bensoussan, A., Lions, J.-L., Papanicolau, G.: Asymptotic Analysis for Periodic Structures. North-Holland, Amsterdam (1978)
24. de Gennes, P.G.: Chemotaxis: the role of internal delays. Eur. Biophys. J. **33**, 691–693 (2004)
25. Attneave, F.: Informational aspects of visual perception. Psychol. Rev. **61**, 183–193 (1954)
26. Barlow, H.B.: Possible principles underlying the transformation of sensory messages. In: Sensory Communication, pp. 217–234. MIT Press, Cambridge (1961)
27. Nemenman, I.: Information theory and adaptation. In: Wall, M.E. (ed.) Quantitative Biology: From Molecular to Cellular Systems. Taylor & Francis, London (2011)
28. Laughlin, S.B.: Form and function in retinal processing. Trends Neurosci. **10**, 478–483 (1987)
29. Brenner, N., Bialek, W., de Ruyter van Steveninck, R.: Adaptive rescaling optimizes information transmission. Neuron **26**, 695–702 (2000)
30. Kalinin, Y.V., Jiang, L., Tu, Y., Wu, M.: Logarithmic sensing in *Escherichia coli* bacterial chemotaxis. Biophys. J. **96**, 2439–2448 (2009)
31. Salman, H., Libchaber, A.: A concentration-dependent switch in the bacterial response to temperature. Nat. Cell Biol. **9**, 1098–1100 (2007)

32. Skoge, M., Endres, R.G., Wingreen, N.S.: Receptor-receptor coupling in bacterial chemotaxis: evidence for strongly-coupled clusters. Biophys. J. **90**, 4317–4326 (2006)
33. Greenfield, D., et al.: Self-organization of the *Escherichia coli* chemotaxis network imaged with super-resolution light microscopy. PLoS Biol. **16**, e1000137 (2009)
34. Manley, S., Gillette, J.M., Patterson, G.H., Shroff, H., Hess, H.F., Betzig, E., Lippincott-Schwartz, J.: High-density mapping of single-molecule trajectories with photoactivated localization microscopy. Nat. Methods **5**, 155–157 (2008)
35. Berg, H.C., Brown, D.A.: Chemotaxis in *Escherichia coli* analysed by three-dimensional tracking. Nature **239**, 500–504 (1972)